Handwriting and Hand Geometry modality experiments

Sasan Haidar Vasim
Study Program DigiEng;M
Immatriculation no. 230089
sasan.haidar@st.ovgu.de

Mohamed Abdelrazek
Study Program INF;M
Immatriculation no. [redacted]
mohamed.abdelrazek@ovgu.de

Abstract

With the growing popularity and prevalence of Biometrics used for authentication and security applications, there exists a wide range of modalities to consider. How they perform based on existing evaluation criteria determines which are well suited for specific use case scenarios. In this report we conduct small scale experiments on two such modalities, namely Handwriting and Hand Geometry, to determine overall performance for an authentication scheme. Based on our results, we concluded that Handwriting is more suited in terms of performance, uniqueness, and circumvention. In our Handwriting experiments, we also recorded two instances of 0% EER for separate semantics used, which indicate high distinguishability. However, our Hand Geometry experiments recorded two EER's of 13.6% and 9% respectively. Even though an extension of our feature space reduced this error rate by a factor of 4.6%, intersection of Intra and Inter class variances leaves room for uncertainty during authentication. Our results were largely dependent on sample sizes used, which was limited due to constricting factors of time. However, it was still sufficient to get an understanding into the performance of our two modalities. We illustrated these results by plotting several EER/FRR/FAR/PDF graphs throughout the report.

Keywords: Equal-Error-Rate (EER), False Rejection Rate (FRR), False Acceptance Rate (FAR), Cumulative Distribution Function (CDF), Probability Distribution Function (PDF).

1. MOTIVATION

In recent years, we have seen vast improvements in technologies that we use every day. These allow us to achieve our goals and solve problems more efficiently. Some of these technologies are everyday computers that we use for work, and devices which are used by many authoritarian bodies. For example, during a passport renewal procedure, multiple biometrics are collected from a data subject. Such devices normally use pins or passwords for security, but to ensure a more secure environment, many of them nowadays utilize biometrics in addition. The majority of these equipment use our biometric data for different tasks, mainly to ensure a safe and error free experience. This in turn raises the concern whether these technologies are secure, and their degree of overall vulnerability. To answer these questions, we attempt a set of small-scale biometric experiments to build a simple authentication system based on two modalities (Handwriting and Hand Geometry). The paper structure is as follows: In Section 2 we introduce our first modality (Handwriting), with reference to the phases of the biometrics processing pipeline. We then define and measure our feature vectors, in order to calculate the respective distances between our enrolment and verification samples. Lastly, we briefly summarize the experimental results. Section 3 introduces the second modality (Hand Geometry), and follows a similar structure to that of Section 2. Our paper concludes in Section 4, where we analyze and give a summary of all our observed results. This is also done with respect to the different modalities involved.

2. MODALITY 1: HANDWRITING

This section focuses entirely on our work done for the Handwriting modality, with a reference to the biometric processing pipeline phases outlined in figure 1.

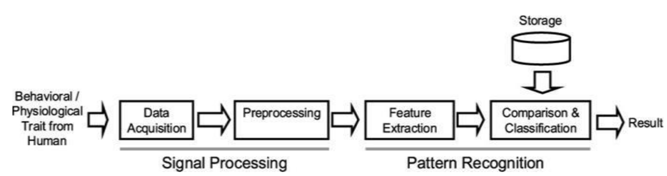

Figure 1: Biometric processing pipeline.

The following subsections detail all aspects of our Data Acquisition, Feature extraction, and Pre-processing steps. Furthermore, the semantics used along with all their evaluation results are outlined in separate subsections, while referencing the forgery attempts exclusively for semantic 2.

2.1 Data Acquisition

When gathering data for our authentication system's enrolment and verification, we used two varying methods.

Student 1 (Sasan) used a paper based approach, wherein all enrolment and verification samples were recorded onto printouts of the grid template provided. Thus, all the existing feature vectors were derived from paper measurements. However, Student 2 (Mohamed) used a tablet based approach for recording all his samples, and as such, the feature values needed to be measured using online tools accordingly (grid-spacing measurement and an online protractor).

2.2 Pre-processing

No pre-processing steps such as outlier removal, normalization, discretization, etc., were applied for our feature distances. Due to the limited number and range of the values, it was in the best interest of the evaluation result for our samples to be as natural as possible. Since none of the feature vectors were abnormally large, pre-processing was not required.

2.3 Feature extraction (Team specific rules)

Before measuring the seven feature vectors from our derived samples, we were tasked with defining team specific rules to avoid any resulting ambiguity when carrying out extraction. The following rules were set for our team:

+ Bounding Box: Our bounding box should encase the surrounding sample text by **2 GRID SPACES** from the outmost coordinate occupied by each angle of the handwriting. An example of this is illustrated in figure 2.

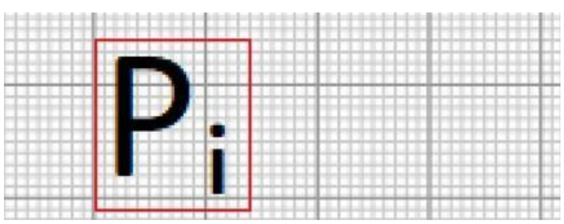

Figure 2: Bounding box representation.

+ Aspect Ratio: We used the formula (BB Width (mm) * 1000 / BB Height (mm) * 1000) to calculate the aspect ratio with respect to the Bounding Box drawn around a sample. Figure 3 illustrates this.

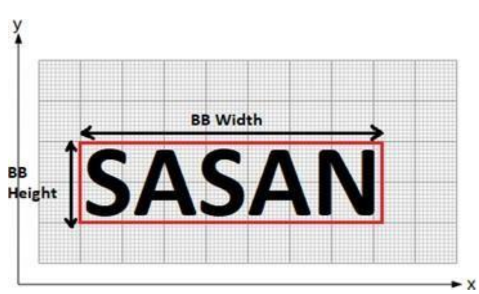

Figure 3: Aspect ratio representation.

+ Segment count: Our segment count is defined as the number of each continuous character line drawn. This also includes isolated points as shown in figure 4. The bridges in the "A" count as separate line segments 8 and 9, whereas the dot in the letter "i" counts as a separate isolated point 6.

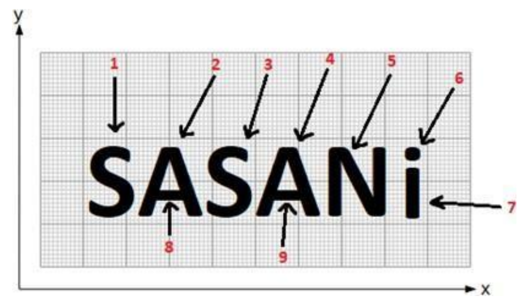

Figure 4: Segment count representation.

+ Baseline angle: This angle is specified as the measured angle between the "Baseline", and the horizontal x-axis. The Baseline is denoted as the dotted line which underlines the sample text's direction. Should the sample text be perfectly horizontal, this angle would be 0°. In the example below, this measured angle is x°.

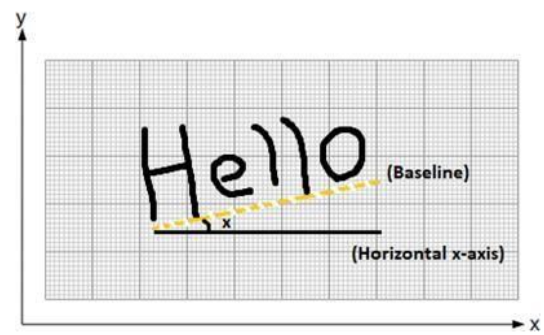

Figure 5: Baseline angle representation.

+ Loop count: Represented as the total number of closed loops in a sample. The loops taken into consideration must only be the result of a continuous character stroke as shown in the example below. The number "2" here is drawn as a continuous segment.

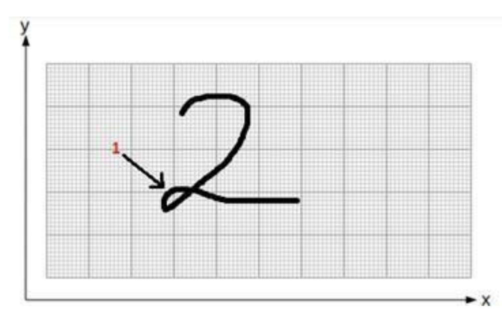

Figure 6: Loop count representation.

+ YMax count: Defined as the total number of vertical local maxima to the y-axis. In figure 7, four points are observed to be in a local maxima position.

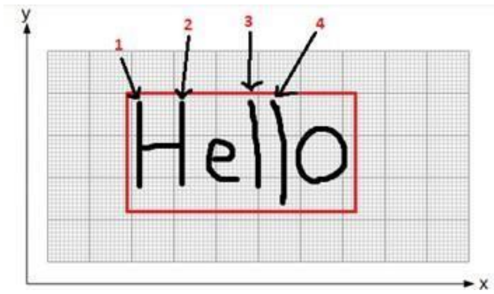

Figure 7: Maxima count representation.

+ YMin count: Defined as the total number of vertical local minima to the y-axis. In the example below, only one point is observed in the local minimum.

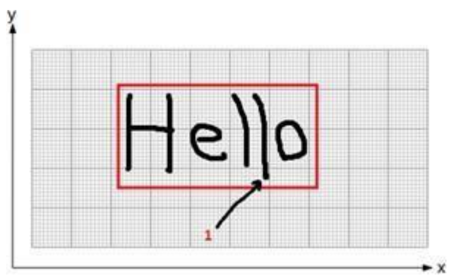

Figure 7: Minima count representation.

+ Intersection count: Defined as the total number of intersections (or crossings) in a sample. An intersection is a point where two or more different strokes (non-continuous) cross paths.

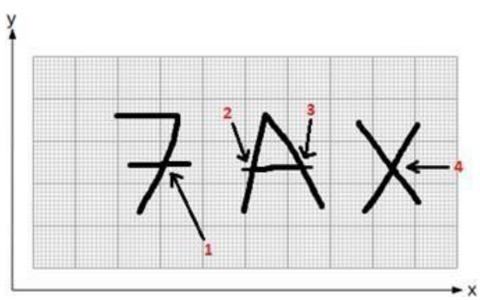

Figure 8: Intersection count representation.

2.4 Semantic 1 (PIN)

As part of the practical work, our authentication system would focus on two semantics separately. This subsection is dedicated to the PIN semantic, which focused on handwriting five enrolment and five verification samples per student, for the number ''77412''. After having measured the feature vectors of all our enrolment and verification samples, we estimated the Euclidean distance between every possible iteration. The resulting distances were then separated into two scatter matrices, each of dimension 10x5. One would represent the Intra-class distances, and the other would be our Inter-class values. These are illustrated in the figures below:

Sasan E1 – Sasan V1

5.57	2.84	3.65	4.13	3.23
3.47	1.01	0.51	3.61	2.32
2.01	2.24	2.87	1.00	1.17
2.01	2.25	2.83	1.08	1.03
3.46	1.00	0.31	3.62	2.27

Mohamed E1 – Mohamed V1

1.03	2.24	2.24	1.08	2.15
3.61	4.05	3.10	2.25	4.15
2.33	2.49	3.07	1.12	3.58
8.53	6.93	10.49	8.16	10.58
3.22	2.31	4.69	2.40	5.01

Figure 9: Intra-class scatter matrices.

Distances in our Intra-class had a varying range, with a relatively big distance between the smallest and largest. In ascending order, we had 50 values in the range [***0.31***, 0.51, 1.0, 1.0, 1.01, 1.03, 1.03, 1.08, 1.08, 1.12, 1.17, 2.01, 2.01, 2.15, 2.24, 2.24, 2.24, 2.25, 2.25, 2.27, 2.31, 2.32, 2.33, 2.4, 2.49, 2.83, 2.84, 2.87, 3.07, 3.1, 3.22, 3.23, 3.46, 3.47, 3.58, 3.61, 3.61, 3.62, 3.65, 4.05, 4.13, 4.15, 4.69, 5.01, 5.57, 6.93, 8.16, 8.53, 10.49, ***10.58***]

Sasan E1 – Mohamed V1

16.9	18.3	14.7	16.7	15.1
15.8	17.4	13.7	15.8	13.9
15.3	17	13	15.2	13.3
15.6	17.2	13.23	15.5	13.6
16	17.5	13.8	16	14.1

Mohamed E1 – Sasan V1

14.5	15.5	15.9	14.6	15.7
14.7	15.7	16.2	14.5	15.7
15.3	16.2	16.6	15.2	16.4
22.6	23.2	23.5	22.5	23.5
17	17.8	18.2	16.9	18

Figure 10: Inter-class scatter matrices.

Similarly, our Inter-class distances varied greatly as well. Having sorted them in ascending order, we had 50 values in the range [***13.0***, 13.23, 13.3, 13.6, 13.7, 13.8, 13.9, 14.1, 14.5, 14.5, 14.6, 14.7, 14.7, 15.1, 15.2, 15.2, 15.3, 15.3, 15.5, 15.5, 15.6, 15.7, 15.7, 15.7, 15.8, 15.8, 15.9, 16.0, 16.0, 16.2, 16.2, 16.4, 16.6, 16.7, 16.9, 16.9, 17.0, 17.0, 17.2, 17.4, 17.5, 17.8, 18.0, 18.2, 18.3, 22.5, 22.6, 23.2, 23.5, ***23.5***]

For drafting the cumulative and probability density graphs, and in order to later derive the FAR/FRR/EER respectively, we utilized a cumulative frequency table. The full table values for both semantic 1 and 2 are listed in Appendix A, however, it is comprised of the following columns:

RANGE	FREQUENCY	CF	PROBABILITY
Stipulated distance range, for example 0<x<=1...	The number of occurrences of distance values in the stipulated range...	Cumulative frequency of the distances...	Probability density, measured as (frequency/total population number) ...

Table 1: Cumulative frequency columns.

Having done so, we then generated the resulting graphs:

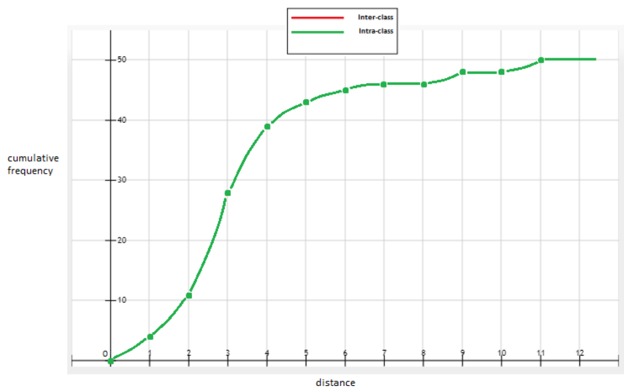

Figure 11: Intra-class CDF, x-axis step = 1, y-axis step = 10.

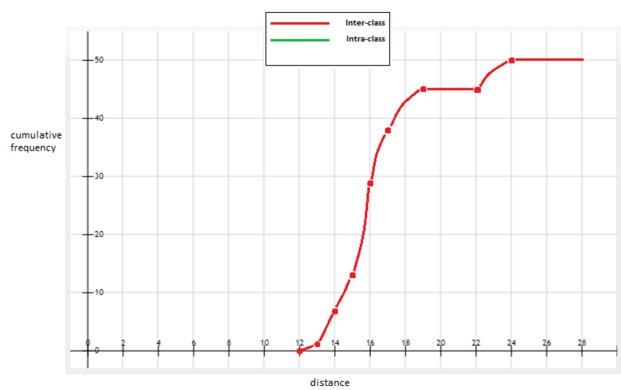

Figure 12: Inter-class CDF, x-axis step = 2, y-axis step = 10.

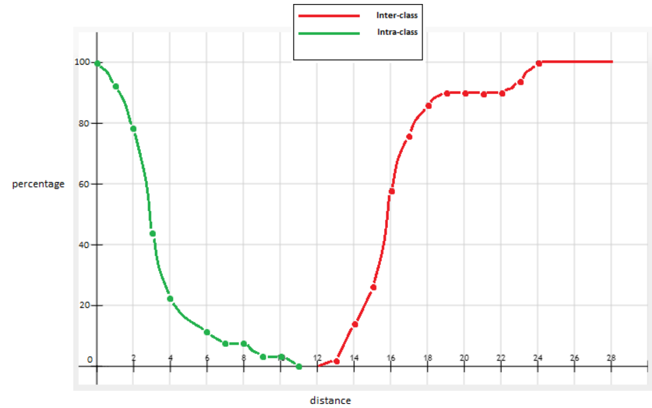

Figure 13: EER graph, x-axis step = 2, y-axis step = 20.

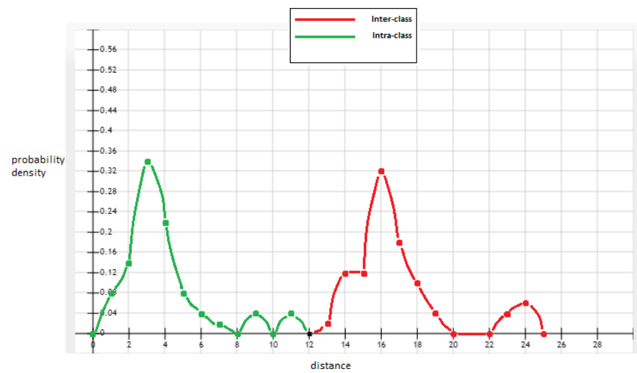

Figure 14: Intra and Inter class PDF, x-axis step = 2, y-axis step = 0.04.

For the PIN semantic, our EER was estimated at 0%. This implies that within a distance threshold range, our authentication system makes no false acceptances nor false rejections. From the EER graph, this threshold is not clearly visible due to plotting steps in the x-axis, however, by reading the highest Intra-class distance and the smallest Inter-class distance, this identified range lies within ***10.58 < x < 13.0***. The resulting performance of our system is largely a consequence of heterogeneous data acquisition, contrasting writing styles, and an overall low sample size to work with.

2.5 Semantic 2 (CITY)

For the second part of our practical work, we were tasked to handwrite our birthplace as five enrolment and verification samples per student. Similar to the methodology used for the PIN semantic, we estimated the feature vectors and subsequent distances, having then drafted two scatter matrices each of dimension 10x5. These are illustrated in the figures below:

Sasan E2 – Sasan V2

3.32	3.61	1	3.16	2.27
1.06	1	3.01	2.02	2.32
1.46	1.41	2.02	2.25	2.10
1.06	1	3.01	2.02	2.32
4.24	5.11	4.47	2.24	2.03

Mohamed E2 – Mohamed V2

2.56	2.08	2.08	1.18	2.13
6.22	9.86	9.86	8.68	6.22
2	3.51	3.51	2.69	2.45
3.20	1.20	1.20	1.41	2.87
3.91	2.24	2.24	2.83	4.39

Figure 15: Intra-class scatter matrices.

Identical to the previous semantic, distances in our Intra-class had a varying range, with a wide distance between the smallest and largest. In ascending order, we accumulated 50 values: [***1.0***, 1.0, 1.0, 1.06, 1.06, 1.18, 1.2, 1.2, 1.41, 1.41, 1.46, 2.0, 2.02, 2.02, 2.02, 2.03, 2.08, 2.08, 2.1, 2.13, 2.24, 2.24, 2.24, 2.25, 2.27, 2.32, 2.32, 2.45, 2.56, 2.69, 2.83, 2.87, 3.01, 3.01, 3.16, 3.2, 3.32, 3.51, 3.51, 3.61, 3.91, 4.24, 4.39, 4.47, 5.11, 6.22, 6.22, 8.68, 9.86, ***9.86***]

Sasan E2 – Mohamed V2

15.8	12.8	12.8	14	16.1
15	11.6	11.6	12.8	15.1
15	11.7	11.7	13	15.2
15	11.6	11.6	12.8	15.1
17	14.1	14.1	15.1	17.1

Mohamed E2 – Sasan V2

13.5	12.9	14	14.3	14.7
21	20.4	21.2	21.4	21.8
14.2	13.6	14.7	15	15.4
13	12.3	13.4	13.8	14.2
12	11.2	12	12.8	13.1

Figure 16: Inter-class scatter matrices.

As such, our Inter-class distances had a noticeable gap as well, more so than the respective Intra-class variance. Sorting them in ascending order we have 50 values in the range [***11.2***, 11.6, 11.6, 11.6, 11.6, 11.7, 11.7, 12.0, 12.0, 12.3, 12.8, 12.8, 12.8, 12.8, 12.8, 12.9, 13.0, 13.0, 13.1, 13.4, 13.5, 13.6, 13.8, 14.0, 14.0, 14.1, 14.1, 14.2, 14.2, 14.3, 14.7, 14.7, 15.0, 15.0, 15.0, 15.0, 15.1, 15.1, 15.1, 15.2, 15.4, 15.8, 16.1, 17.0, 17.1, 20.4, 21.0, 21.2, 21.4, ***21.8***]

Consistent with our methodology from part one, we reused the cumulative frequency table (see table 1) to plot the CDF/PDF, and subsequently projected the FAR/FRR/EER respectively. Our resulting graphs are as follows:

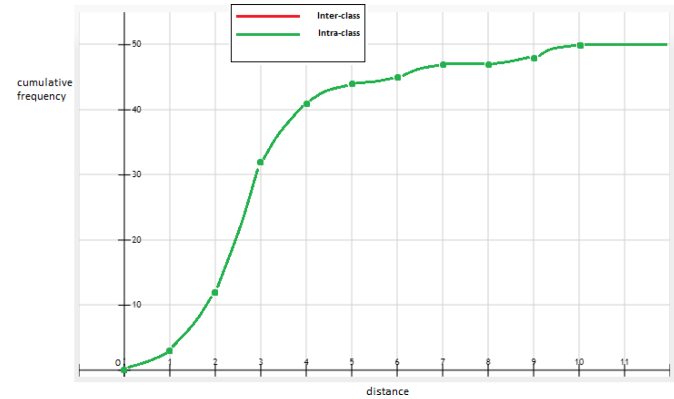

Figure 17: Intra-class CDF, x-axis step = 1, y-axis step = 10.

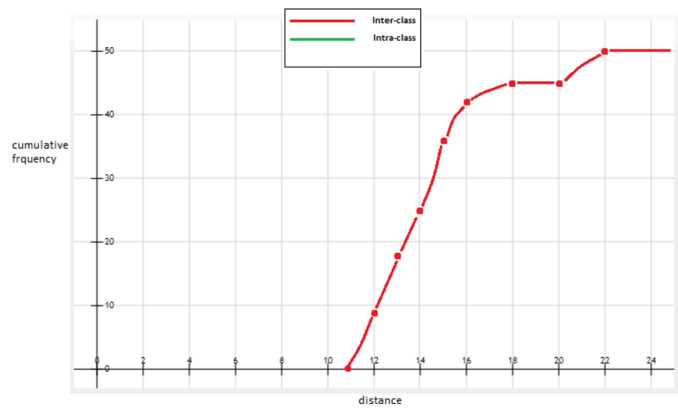

Figure 18: Inter-class CDF, x-axis step = 2, y-axis step = 10.

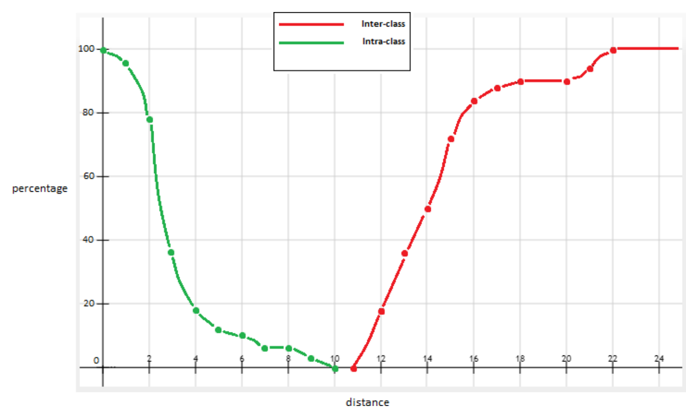

Figure 19: EER graph, x-axis step = 2, y-axis step = 20.

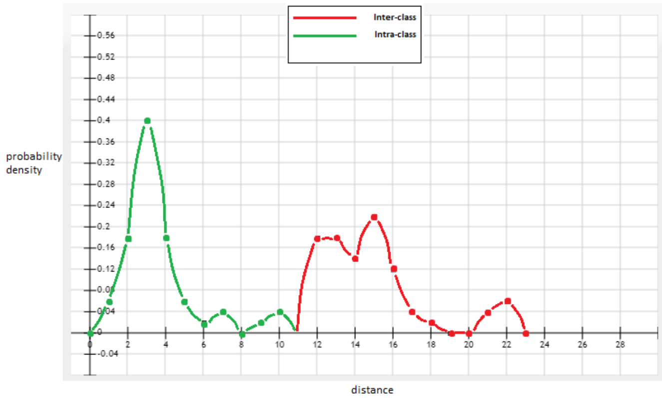

Figure 20: Intra and Inter class PDF, x-axis step = 2, y-axis step = 0.04.

From analyzing the EER graph, our equal error rate is 0%. This indicates total separation between false acceptances and false rejections, at an estimated distance threshold range. To precisely identify this, we take the largest Intra-class distance, and the smallest Inter-class distance, which lies within **9.86 < x < 11.2**. Since our projected results are similar to that of the PIN semantic, the underlying reasons are the same as well (different data acquisition approaches, high contrast in our writing styles, and small sample size used).

2.5.1 Forgeries

Additionally, for semantic two we were also tasked to extend our system's performance by using forgery samples. We carried this out using **two** knowledge levels, with **one** forgery sample produced per student at each respective level. In **Knowledge level 1**, we verbally told each other our birthplaces, and then produced a forgery sample based on that. Having measured the feature vectors with respect to our team specific rules, we then measured the Euclidean distance between each enrolment and forgery (verification) sample. Our scatter matrices are as follows for Knowledge level 1:

SASAN E – MOHAMED V	MOHAMED E – SASAN V
14.6	14.3
13.5	21.9
13.6	15
13.5	13.8
15.8	12.7

Figure 21: Forgery scatter matrices K1.

With respect to the 10 distance values, we ordered them in the range [***12.7***, 13.5, 13.5, 13.6, 13.8, 14.3, 14.6, 15.0, 15.8, ***21.9***], and drafted the following CDF and PDF:

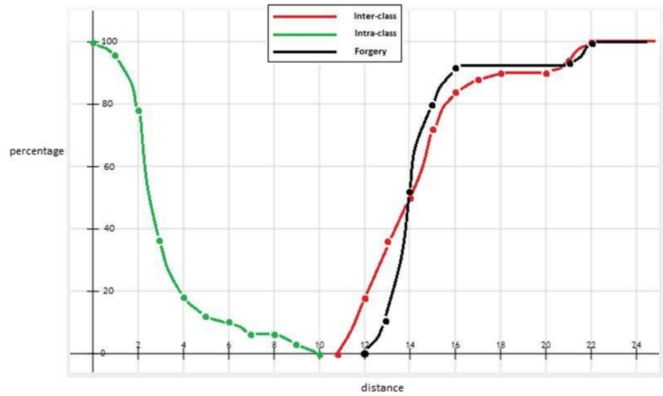

Figure 22: Knowledge level 1, Intra-class CDF/EER, x-axis step = 2, y-axis step = 20.

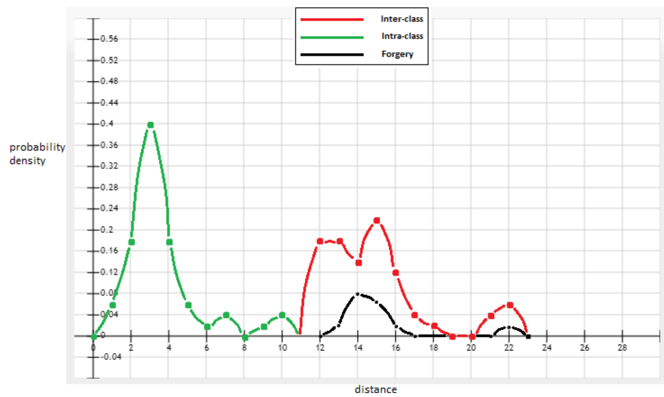

Figure 23: Knowledge level 1, Intra-class PDF, x-axis step = 2, y-axis step = 0.04.

In **Knowledge level 2**, we showed each other our enrolment and verification samples in advance, to better mimic our respective handwriting styles. Resulting scatter matrices are for Knowledge level 2:

SASAN E – MOHAMED V	MOHAMED E – SASAN V
13.5	15.7
13.6	22.9
13.5	16.6
15.8	15.1
14.6	14.5

Figure 24: Forgery scatter matrices K2.

With respect to the 10 distance values, we ordered them in the range [***13.5***, 13.5, 13.6, 14.5, 14.6, 15.1, 15.7, 15.8, 16.6, ***22.9***], and drafted the following CDF and PDF:

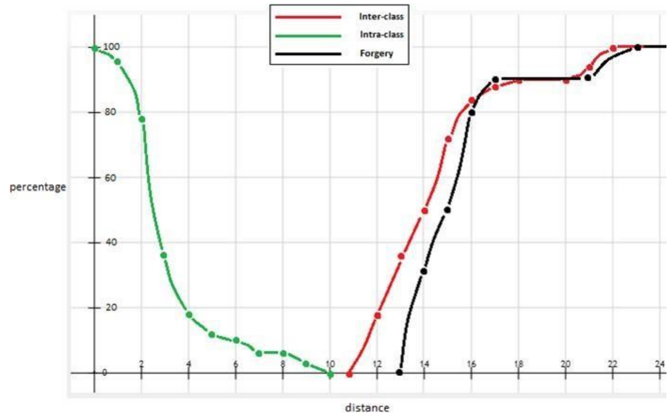

Figure 25: Knowledge level 2, Intra-class CDF/EER, x-axis step = 2, y-axis step = 20.

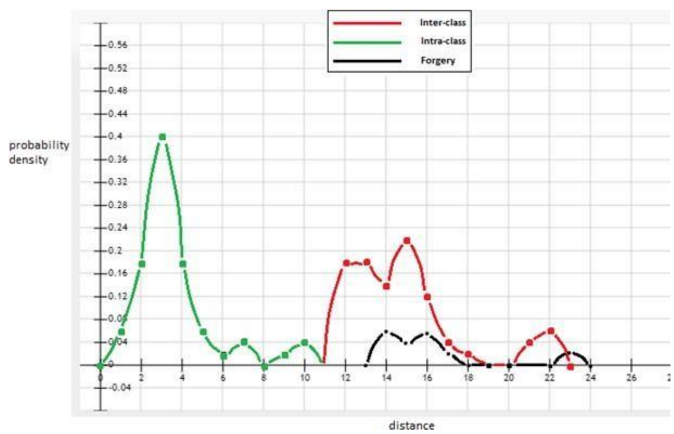

Figure 26: Knowledge level 2, Intra-class PDF, x-axis step = 2, y-axis step = 0.04.

From analyzing the differences between the two EER graphs, our forgery attempts were unsuccessful in closing the gap between the Intra and Inter-class variances respectively. On the other hand, with each increasing knowledge level this gap actually increased (**Inter-class** starting distance **11.2**, **K1 level** starting distance **12.7**, **K2 level** starting distance **13.5**). The resulting performance could be due to the limited sample size we were working with, and/or the number of forgery samples produced per student. Due to time constraints and other factors, we had to limit the number of forgeries to one per student for each knowledge level, and this may have had a negative impact on the performance that was expected. To more adequately verify the impact of forgeries, we would need at least 10-15 samples for each knowledge level with an overall bigger sample size to work with.

All of our recorded enrolment and verification samples for the Handwriting modality are also illustrated in Appendix A, including each forgery sample at different knowledge levels as well.

3. MODALITY 2: HAND GEOMETRY

In this section, we discuss our second chosen modality (Hand geometry). Similarly, we follow the same biometric processing pipeline as in section 2 (Figure 1).

In the following subsections we first discuss our data acquisition procedure, pre-processing steps, and the team defined feature extraction procedures. We divide this modality into two parts, the first using only four pre-defined feature extraction approaches. In the second part we define five more additional features. For each part we also present the evaluation results for both students involved.

3.1 Data Acquisition

Similarly as in section 2.1, we needed to gather enrollment and verification data for our authentication system. Both student 1 (Sasan) and student 2 (Mohamed) used a paper-based approach for obtaining their data. Both students also used pen and plain paper to draw their hand silhouettes respectively. To extract features for the acquired data, both of us used a single ruler only. At the end of each part, we acquired 5 enrollment and 5 verification samples. With respect to finger spacing, we set the rule to place our hands as naturally as possible on the paper, so that the features obtained would be as normal as possible.

3.2 Pre-processing

Similarly as in section 2.2, no other pre-processing approaches were used. This was due to the fact that none of our feature vectors were within an abnormal range.

3.3 Feature extraction (Team specific rules)

In part 1, we were given a pre-defined set of features to be measured using a ruler. Those features are:

A: Distance from the index fingertip to the bottom knuckle.

B: Width of the ring finger, measured across the top knuckle.

C: Width of the palm across the 4 bottom knuckles.

D: Width of the palm, from the middle knuckle of the thumb, across the hand.

All of the defined features are measured using a ruler in centimeters. Figure 27 shows a visual representation of how the features are extracted.

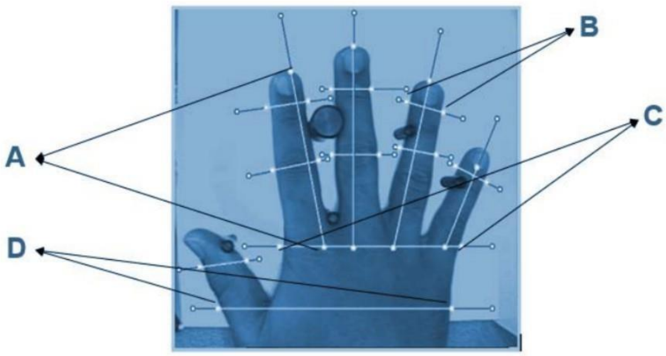

Figure 27: A visual representation of the given pre-defined features to be measured.

In part 2, we were asked to expand our feature set with five additional features, to also be measured following the same procedure as the pre-defined set. We tried to extend our feature space by adding simple features (e.g. by avoiding calculating angles between fingers) so that we do not worsen our equal error rate. These extended features are:

E: Width of the middle finger, measured across the top knuckle.

F: Width of the pinkie, measured across the top knuckle.

G: Distance from the middle fingertip to the bottom knuckle.

H: Distance from the ring fingertip to the bottom knuckle.

I: Distance from the pinkie fingertip to the bottom knuckle.

Figure 28 shows a visualization of these extended features.

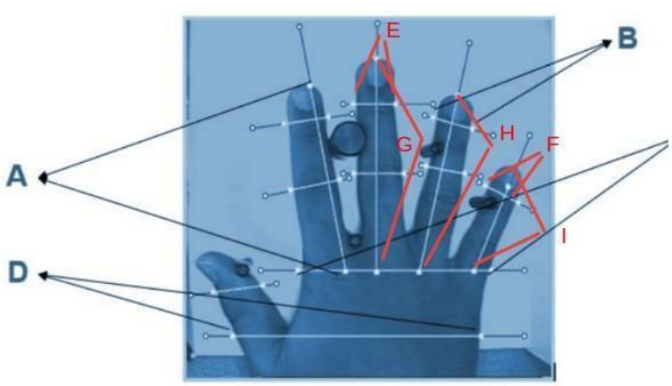

Figure 28: A visual representation of the given pre-defined features, and the extended set of features to be measured for part 2.

3.4 Part 1

In this section we focus on part 1 of our Hand Geometry authentication system, which uses the set of pre-defined given features only. Similarly as in the first modality, each student acquired the data for enrollment and verification (5 samples each) and measured their feature vectors respectively. Then, each student measured the Euclidean distances between both their enrollment and verification matrices, which are represented by the Intra and Inter class matrix. These are shown in figures 29 and 30.

SASAN E1 - SASAN V1

1.19	1.14	0.81	1.13	1.35
0.46	0.63	0.2	0.26	0.42
0.22	0.39	0.22	0.9	0.74
0.39	0.54	0.29	0.29	0.47
0.3	0.27	0.4	0.62	0.9

MOHAMED E1 - MOHAMED V1

1.41	1.41	1.73	1.41	1.73
2	2.45	1	0	1
1.41	2	1	1.41	1
1.73	2.24	0	1	0
1	1	1.41	1.73	1.41

Figure 29: Intra-class scatter matrices.

Our Intra-class scatter matrices for part 1 have a low varying range of values, with relatively low distances. The minimum value being 0, and the highest 2.45. This can be seen when re-arranging the 50 values of both Intra-class matrices, in ascending order as follows: [***0.0***, 0.0, 0.0, 0.2, 0.22, 0.22, 0.26, 0.27, 0.29, 0.29, 0.3, 0.39, 0.39, 0.4, 0.42, 0.46, 0.47, 0.54, 0.62, 0.63, 0.74, 0.81, 0.9, 0.9, 1.0, 1.0, 1.0, 1.0, 1.0, 1.0, 1.0, 1.13, 1.14, 1.19, 1.35, 1.41, 1.41, 1.41, 1.41, 1.41, 1.41, 1.41, 1.73, 1.73, 1.73, 1.73, 2.0, 2.0, 2.24, ***2.45***].

Similarly as in the first modality, we also calculated the Inter-class matrices for the Hand Geometry modality, which is shown in figure 30.

SASAN E1 - MOHAMED V1

2.9	2.8	1.5	1.3	1.5
3.5	3.4	1.9	1.8	1.9
3.3	3.3	1.6	1.6	1.6
3.6	3.6	2.1	1.9	2.1
3.3	3.4	1.8	1.6	1.8

MOHAMED E1 - SASAN V1

2.9	2.7	2.8	3.1	3.1
1.7	1.6	1.8	2.1	2.2
2.4	2.3	2.6	2.8	3
1.8	1.8	2	2.2	2.4
3	2.9	2.9	3.2	3.2

Figure 30: Inter-class scatter matrices.

Like the Intra-class matrices, our Inter-class matrices have relatively low distance values. The lowest value being 1.3, and the highest value 3.6. This is shown when re-arranging the values in ascending order as follows: [***1.3***, 1.5, 1.5, 1.6, 1.6, 1.6, 1.6, 1.6, 1.7, 1.8, 1.8, 1.8, 1.8, 1.8, 1.8, 1.9, 1.9, 1.9, 2.0, 2.1, 2.1, 2.1, 2.2, 2.2, 2.3, 2.4, 2.4, 2.6, 2.7, 2.8, 2.8, 2.8, 2.9, 2.9, 2.9, 2.9, 3.0, 3.0, 3.1, 3.1, 3.2, 3.2, 3.3, 3.3, 3.3, 3.4, 3.4, 3.5, 3.6, ***3.6***].

For calculating the cumulative and probability density graphs (CDF and PDF respectively), we used the same cumulative frequency table for guidance, as in the first modality. All detailed values are available in Appendix A for reference.

We then calculated and plotted both the Intra-class and Inter-class CDF's, as well as the EER graph and PDF's. With respect to figures 31, 33 and 34, negative distance values are a result of plotting consistencies in the x-axis. Multiple values were at a distance of 0, and in order to preserve consistency of the cumulative frequency table and a gaussian curve, we allowed negative plotting in this instance only.

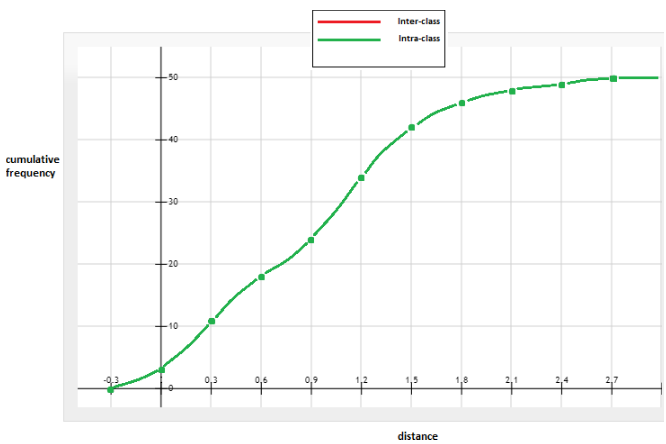

Figure 31: Intra-class CDF, x-axis step = 0.3, y-axis step = 10.

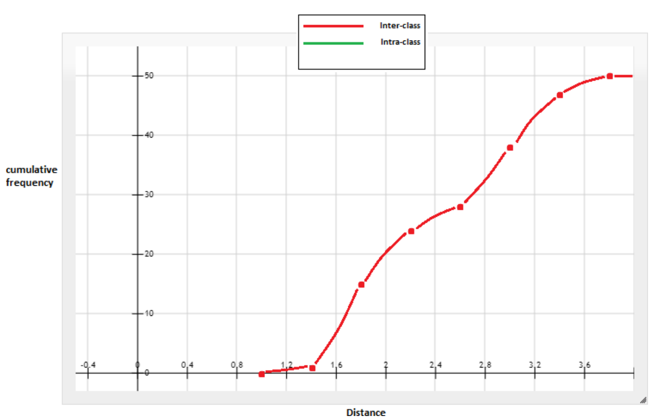

Figure 32: Inter-class CDF, x-axis step = 0.4, y-axis step = 10.

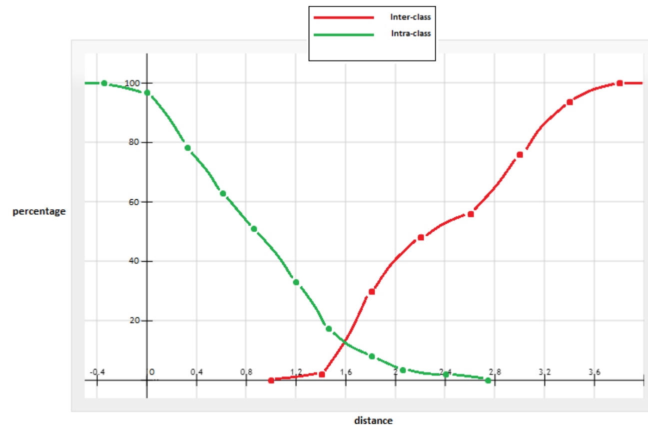

Figure 33: EER graph, x-axis step = 0.4, y-axis step = 20.

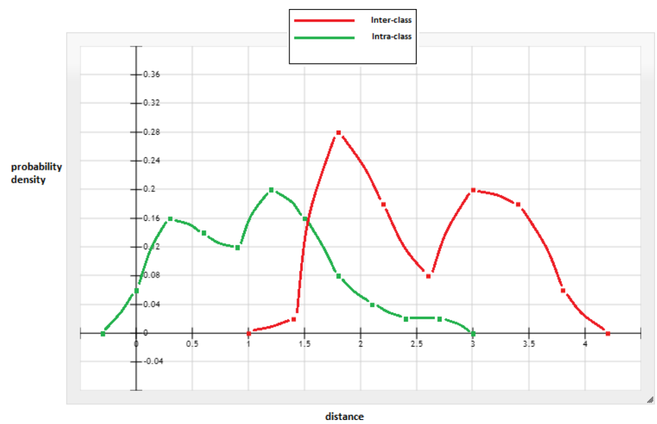

Figure 34: Intra and Inter class PDF, x-axis step = 0.5, y-axis step = 0.04.

From analyzing our EER graph for part 1, we can observe that our equal error rate is 13.6% at a distance threshold of 1.58. Unlike our first modality (Handwriting), we can see that our authentication system has some errors, and both the Intra and Inter-class graphs intersect (as shown in figure 33). This gives us the chance to improve our performance in part 2, where we plan to add newly defined features to our existing feature space, and analyze it's impact on the EER.

3.5 Part 2

In the second part of our Hand Geometry experiment, we will use the extended feature set to observe what kind of impact they have on the error rate calculated in part 1. Whether they improve or worsen our system's performance is key to determining the quality of new features used.

Similarly as in part 1, we calculated first the Intra-class matrices shown in figure 35.

SASAN E2 - SASAN V2

1.5	1.6	1.1	1.3	1.4
1.2	1.4	0.7	0.9	1.1
1	1.2	0.6	0.9	1.1
1	1.2	0.7	0.7	0.9
0.7	0.8	0.8	0.8	1

MOHAMED E2 - MOHAMED V2

2	2	2.2	2.5	2.2
2.2	2.2	1.4	1.7	2
2	1.4	1.7	2	1.7
2.2	1.7	1.4	1.7	1.4
1.4	1.4	1.7	2.5	2.2

Figure 35: Intra-class scatter matrices.

From observing the Intra-class distances, we can see that the values have a low varying range, with an average distance between both the smallest and largest value. This can be seen here: [***0.6***, 0.7, 0.7, 0.7, 0.7, 0.8, 0.8, 0.8, 0.9, 0.9, 0.9, 1.0, 1.0, 1.0, 1.1, 1.1, 1.1, 1.2, 1.2, 1.2, 1.3, 1.4, 1.4, 1.4, 1.4, 1.4, 1.4, 1.4, 1.4, 1.5, 1.6, 1.7, 1.7, 1.7, 1.7, 1.7, 1.7, 2.0, 2.0, 2.0, 2.0, 2.0, 2.2, 2.2, 2.2, 2.2, 2.2, 2.2, 2.5, 2.5].

We also calculated the Inter-class matrices, as shown in figure 36.

SASAN E2 - MOHAMED V2

3.2	3	2.6	2.1	2.1
3.8	3.6	3.1	2.5	2.3
3.5	3.6	2.8	2.3	2.2
4	3.9	3.3	2.6	2.6
3.7	3.7	3.1	2.3	2.5

MOHAMED E2 - SASAN V2

3.9	3.9	3.5	3.8	4
2.8	2.9	2.5	2.8	3
3.2	3.2	3	3.2	3.5
2.7	2.8	2.4	2.7	2.9
4	4	3.6	3.9	4.1

Figure 36: Inter-class scatter matrices.

As in part 1, we also observed a varying range of Inter-class distance values. Additionally, we also see a slight increase between our highest and lowest distance values, when compared to part 1. [***2.1***, 2.1, 2.2, 2.3, 2.3, 2.3, 2.4, 2.5, 2.5, 2.5, 2.6, 2.6, 2.6, 2.7, 2.7, 2.8, 2.8, 2.8, 2.8, 2.9, 2.9, 3.0, 3.0, 3.0, 3.1, 3.1, 3.2, 3.2, 3.2, 3.2, 3.3, 3.5, 3.5, 3.5, 3.6, 3.6, 3.6, 3.7, 3.7, 3.8, 3.8, 3.9, 3.9, 3.9, 3.9, 4.0, 4.0, 4.0, 4.0, ***4.1***].

With the aid of our cumulative frequency table (table 1), we plotted our CDF and PDF graphs respectively.

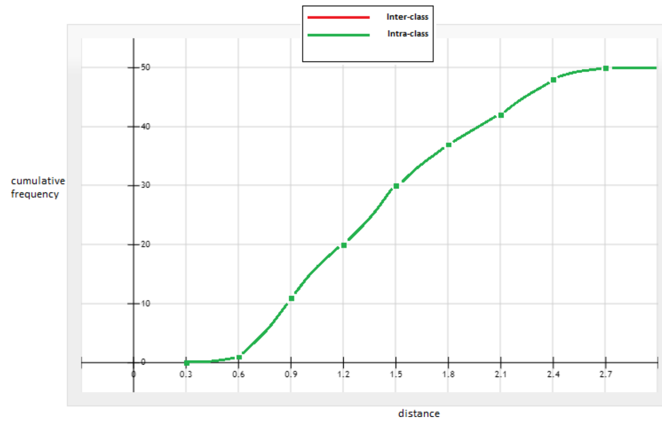

Figure 37: Intra-class CDF, x-axis step = 0.3, y-axis step = 10.

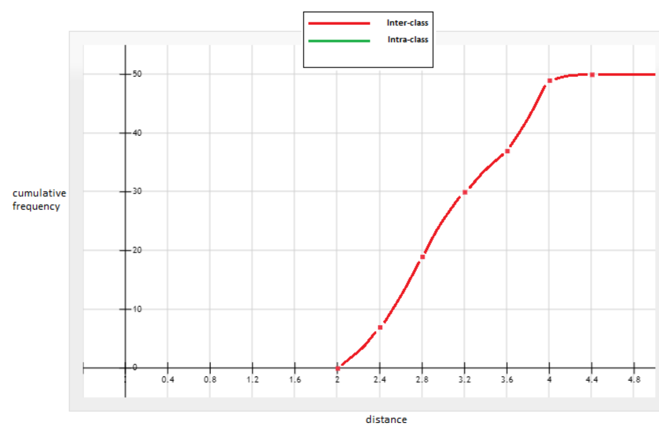

Figure 38: Inter-class CDF, x-axis step = 0.4, y-axis step = 10.

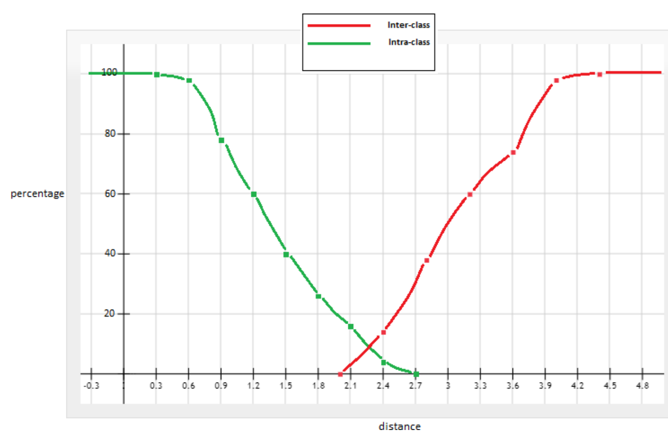

Figure 39: EER graph, x-axis step = 0.3, y-axis step = 20.

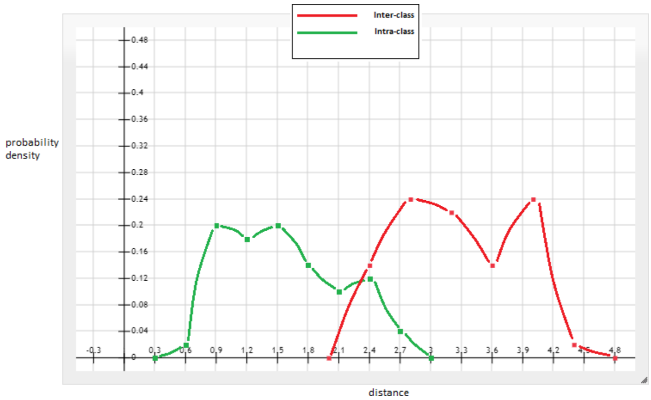

Figure 40: EER graph, x-axis step = 0.3, y-axis step = 0.04.

From analysis of the graph in figure 40, our EER is 9% at a distance threshold of 2.27. This result indicates that the newly added features to our feature space improved our authentication system by reducing the EER. Thus, by the addition of these new features, our overall system performance improved as well.

4. SUMMARY OF THE RESULTS AND COMPARISON OF BOTH MODALITIES

4.1 PIN and CITY semantic (Handwriting)

Both of our semantics achieved an EER of 0%. For the PIN, this was at a distance threshold of **10.58 < x < 13.0**. With respect to the CITY semantic, this threshold was in the range of **9.86 < x < 11.2** respectively. In terms of performance, this meant our system was able to adequately distinguish our handwritings from one another, mainly due to our distinct writing styles and different data acquisition approaches. However, the separation of Intra and Inter classes could have been greater (better performance), but was prevented due to large and isolated Intra class distances from Mohamed. These are illustrated in row 4 (PIN), and row 2 (CITY) of our scatter matrices in figure 41.

MOAHMED E1 - MOHAMED V1 (PIN)

1.03	2.24	2.24	1.08	2.15
3.61	4.05	3.10	2.25	4.15
2.33	2.49	3.07	1.12	3.58
8.53	6.93	10.49	8.16	10.58
3.22	2.31	4.69	2.40	5.01

MOHAMED E2 - MOHAMED V2 (CITY)

2.56	2.08	2.08	1.18	2.13
6.22	9.86	9.86	8.68	6.22
2	3.51	3.51	2.69	2.45
3.20	1.20	1.20	1.41	2.87
3.91	2.24	2.24	2.83	4.39

Figure 41: Intra class matrix anomalies.

Other than this, no further anomalies were identified in our handwriting modality.

4.2 Forgeries

Our forgery attempts for the CITY semantic were unsuccessful in closing the gap between our Intra and Inter class variances. The starting distance was 11.2, and at Knowledge level 1, this became 12.7, which in turn further increased to 13.5 at Knowledge level 2. This indicates the opposite of what we were aiming to achieve, as shown by the increasing gap with each increment of our knowledge level. With respect to this analysis we classified our roles onto the Doddingtons Zoo [2] concept as follows:

+ **Wolf**: Neither of us were Wolves, since both of us were unable to easily impersonate one another.

+ **Lamb**: Neither of us were Lambs, since none of us were vulnerable to being easily impersonated.

+ **Goat**: Neither of us were Goats, since the system did not have a hard time identifying either one of us (no high false-match rates).

+ **Sheep**: We were both classified as Sheep, due to the existing separation of Intra and Inter class variances. This meant we were readily identifiable by the system.

SHEEP (sasan, mohamed)	GOAT
LAMB	WOLF

Figure 42: Doddington's Zoo classification.

4.3 Hand Geometry

In part 1 of our second modality, we were able to achieve an EER of 13.6% at a distance threshold of 1.58. This performance was based on the 4 existing pre-defined feature rules (explained in figure 27). In part 2, we managed to reduce our previous EER to 9% at a distance threshold of 2.27, with the aid of our newly introduced feature rules (explained in figure 28). This indicates an improvement in overall performance by a factor of 4.6%, which classifies the use of our extended feature space as justifiable.

4.4 Handwriting vs Hand Geometry

By analyzing each part of our modalities and comparing them with respect to one another, we came to the following conclusions:

+ Handwriting has a higher degree of uniqueness and performance: Comparing the EER of 0% to 13.6% and 9%

respectively, shows a greater amount of uniqueness and performance for modality 1.

+ Handwriting is hard to forge: This is a consequence of our forgery results. Even though we produced one sample each at different knowledge levels, it is hard to sufficiently circumvent this modality.

+ Extension of feature rules is subjective to performance: With the aid of properly defined feature rules, we were able to improve our Hand Geometry's performance. However, this was highly dependent on the quality of feature rules used, which if improper, could have decreased overall performance as a consequence.

5. LITERATURE & FURTHER SOURCES

[1] Kraetzer, C., and Dittmann, J. 2021. Student task description. Course "Biometrics and Security" - Winter term '21 / '22. Otto-von-Guericke University of Magdeburg, Dept. of Computer Science, 2021.

[2] Teli, Mohammad Nayeem, et al. "Biometric zoos: Theory and experimental evidence." 2011 International Joint Conference on Biometrics (IJCB). IEEE, 2011.

APPENDIX A – DOCUMENTATION OF THE DATA GENERATED / USED AND MECHANISMS USED TO ENSURE ITS PRIVACY

1.0 HANDWRITING MODALITY

1.1 Sasan Enrolment and Verification samples

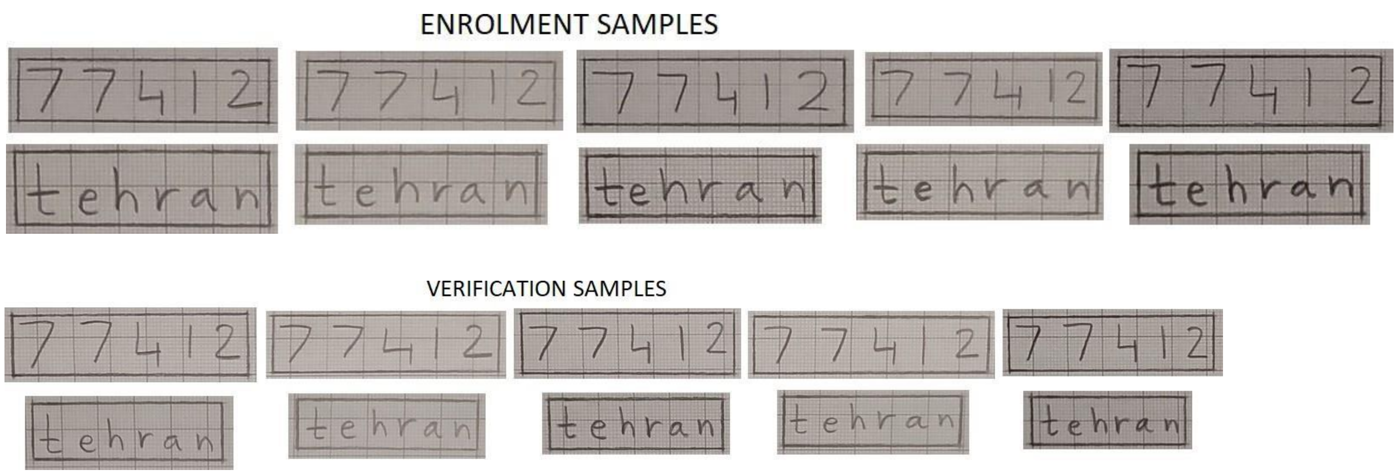

1.2 Mohamed Enrolment and Verification samples

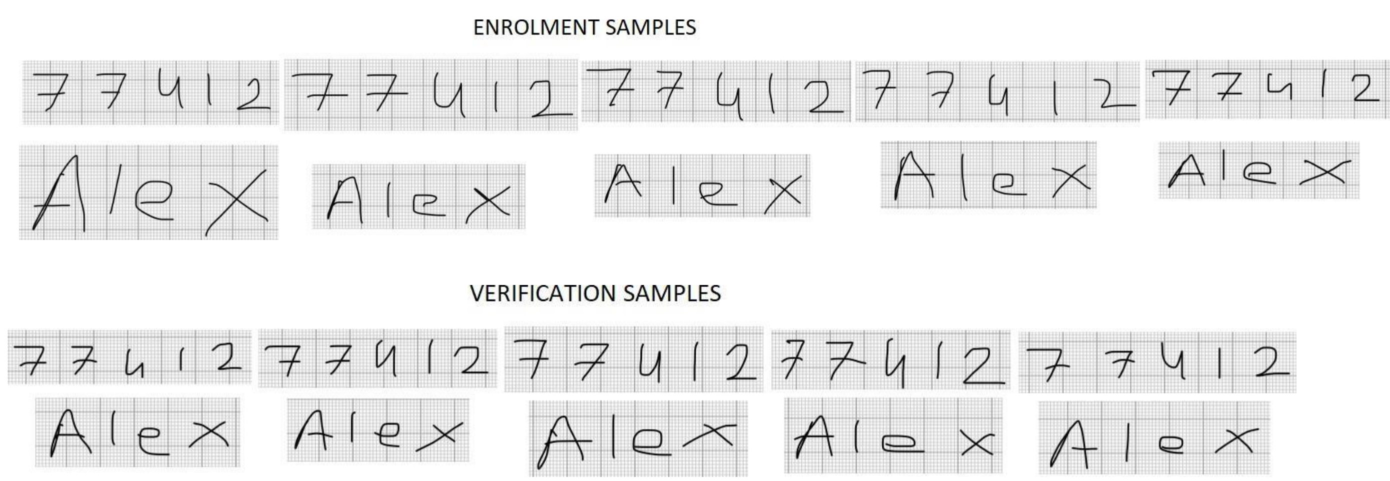

1.3 Semantic 1 (Scatter matrices, Cumulative frequency table)

Intra-class matrix

Sasan E1 – Sasan V1

5.57	2.84	3.65	4.13	3.23
3.47	1.01	0.51	3.61	2.32
2.01	2.24	2.87	1.00	1.17
2.01	2.25	2.83	1.08	1.03
3.46	1.00	0.31	3.62	2.27

Mohamed E1 – Mohamed V1

1.03	2.24	2.24	1.08	2.15
3.61	4.05	3.10	2.25	4.15
2.33	2.49	3.07	1.12	3.58
8.53	6.93	10.49	8.16	10.58
3.22	2.31	4.69	2.40	5.01

Inter-class matrix

Sasan E1 – Mohamed V1

16.9	18.3	14.7	16.7	15.1
15.8	17.4	13.7	15.8	13.9
15.3	17	13	15.2	13.3
15.6	17.2	13.23	15.5	13.6
16	17.5	13.8	16	14.1

Mohamed E1 – Sasan V1

14.5	15.5	15.9	14.6	15.7
14.7	15.7	16.2	14.5	15.7
15.3	16.2	16.6	15.2	16.4
22.6	23.2	23.5	22.5	23.5
17	17.8	18.2	16.9	18

Cumulative Frequency Table (INTRA-CLASS)

Range	Frequency	CF	Probability
0<x<=1	4	4	0.08
1<x<=2	7	11	0.14
2<x<=3	17	28	0.34
3<x<=4	11	39	0.22
4<x<=5	4	43	0.08
5<x<=6	2	45	0.04
6<x<=7	1	46	0.02
7<x<=8	0	46	0
8<x<=9	2	48	0.04
9<x<=10	0	48	0
10<x<=11	2	50	0.04

Cumulative Frequency Table (INTER-CLASS)

Range	Frequency	CF	Probability
12<x<=13	1	1	0.02
13<x<=14	6	7	0.12
14<x<=15	6	13	0.12
15<x<=16	16	29	0.32
16<x<=17	9	38	0.18
17<x<=18	5	43	0.1
18<x<=19	2	45	0.04
19<x<=20	0	45	0
20<x<=21	0	45	0
21<x<=22	0	45	0
22<x<=23	2	47	0.04
23<x<=24	3	50	0.06

1.4 Semantic 2 (Scatter matrices, Cumulative frequency table)

Intra-class matrix

Sasan E2 – Sasan V2

3.32	3.61	1	3.16	2.27
1.06	1	3.01	2.02	2.32
1.46	1.41	2.02	2.25	2.10
1.06	1	3.01	2.02	2.32
4.24	5.11	4.47	2.24	2.03

Mohamed E2 – Mohamed V2

2.56	2.08	2.08	1.18	2.13
6.22	9.86	9.86	8.68	6.22
2	3.51	3.51	2.69	2.45
3.20	1.20	1.20	1.41	2.87
3.91	2.24	2.24	2.83	4.39

Inter-class matrix

Sasan E2 – Mohamed V2

15.8	12.8	12.8	14	16.1
15	11.6	11.6	12.8	15.1
15	11.7	11.7	13	15.2
15	11.6	11.6	12.8	15.1
17	14.1	14.1	15.1	17.1

Mohamed E2 – Sasan V2

13.5	12.9	14	14.3	14.7
21	20.4	21.2	21.4	21.8
14.2	13.6	14.7	15	15.4
13	12.3	13.4	13.8	14.2
12	11.2	12	12.8	13.1

Cumulative Frequency Table (INTRA-CLASS)

Range	Frequency	CF	Probability
0<x<=1	3	3	0.06
1<x<=2	9	12	0.18
2<x<=3	20	32	0.4
3<x<=4	9	41	0.18
4<x<=5	3	44	0.06
5<x<=6	1	45	0.02
6<x<=7	2	47	0.04
7<x<=8	0	47	0
8<x<=9	1	48	0.02
9<x<=10	2	50	0.04

Cumulative Frequency Table (INTER-CLASS)

Range	Frequency	CF	Probability
11<x<=12	9	9	0.18
12<x<=13	9	18	0.18
13<x<=14	7	25	0.14
14<x<=15	11	36	0.22
15<x<=16	6	42	0.12
16<x<=17	2	44	0.04
17<x<=18	1	45	0.02
18<x<=19	0	45	0
19<x<=20	0	45	0
20<x<=21	2	47	0.04
21<x<=22	3	50	0.06

1.4.1 Forgeries (samples, cumulative frequency tables)

FORGERY SAMPLES KNOWLEDGE LEVEL 1

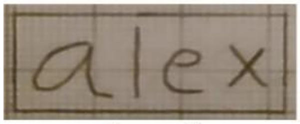

(sasan)

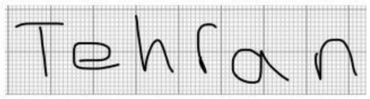

(mohamed)

Cumulative Frequency Table K1 (INTER-CLASS)

Range	Frequency	CF	Probability
12<x<=13	1	1 (x5)	0.02
13<x<=14	4	5 (x5)	0.08
14<x<=15	3	8 (x5)	0.06
15<x<=16	1	9 (x5)	0.02
16<x<=17	0	9 (x5)	0
17<x<=18	0	9 (x5)	0
18<x<=19	0	9 (x5)	0
19<x<=20	0	9 (x5)	0
20<x<=21	0	9 (x5)	0
21<x<=22	1	10 (x5)	0.02

FORGERY SAMPLES KNOWLEDGE LEVEL 2

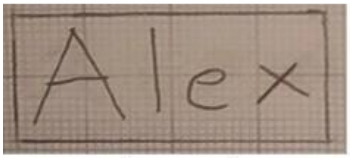

(sasan)

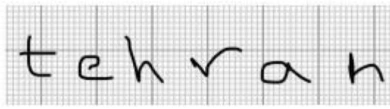

(mohamed)

Cumulative Frequency Table K2 (INTER-CLASS)

Range	Frequency	CF	Probability
13<x<=14	3	3 (x5)	0.06
14<x<=15	2	5 (x5)	0.04
15<x<=16	3	8 (x5)	0.06
16<x<=17	1	9 (x5)	0.02
17<x<=18	0	9 (x5)	0
18<x<=19	0	9 (x5)	0
19<x<=20	0	9 (x5)	0
20<x<=21	0	9 (x5)	0
21<x<=22	0	9 (x5)	0
22<x<=23	1	10 (x5)	0.02

2.0 HAND GEOMETRY MODALITY

2.1 Sasan enrolment and verification samples

ENROLMENT SAMPLES

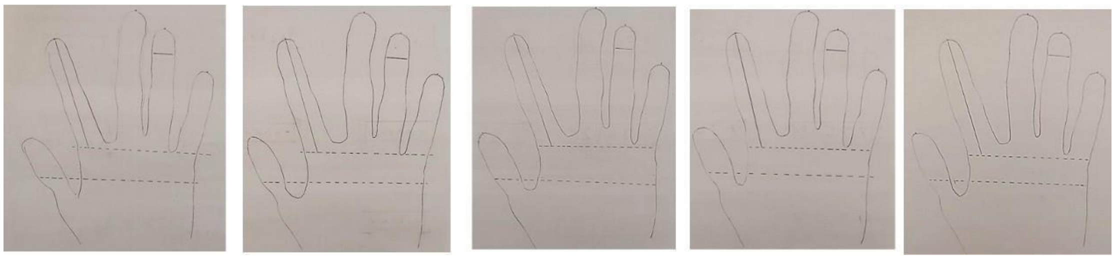

VERIFICATION SAMPLES

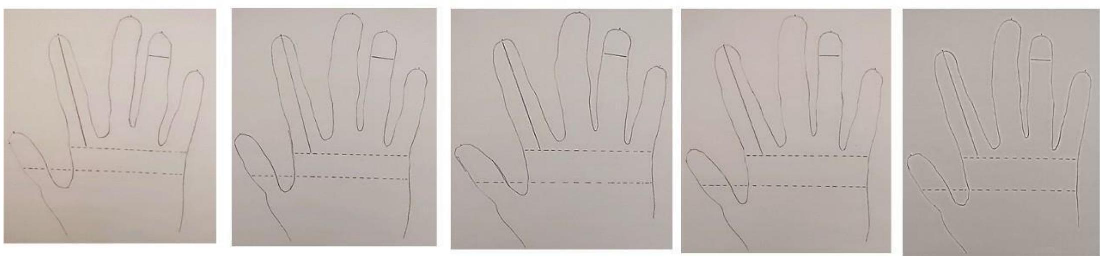

2.2 Mohamed enrolment and verification samples

ENROLMENT SAMPLES

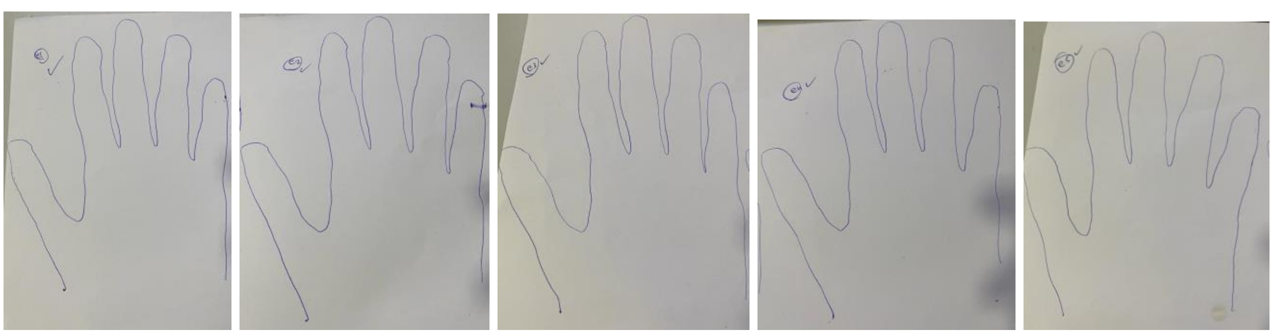

VERIFICATION SAMPLES

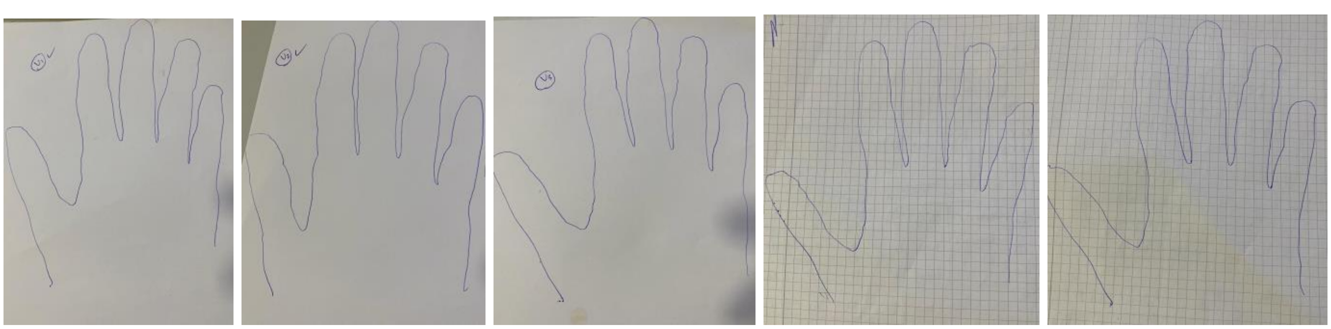

2.3 Part 1 (Scatter matrices, Cumulative frequency table)

Intra-class matrix

1.19	1.14	0.81	1.13	1.35
0.46	0.63	0.2	0.26	0.42
0.22	0.39	0.22	0.9	0.74
0.39	0.54	0.29	0.29	0.47
0.3	0.27	0.4	0.62	0.9

1.41	1.41	1.73	1.41	1.73
2	2.45	1	0	1
1.41	2	1	1.41	1
1.73	2.24	0	1	0
1	1	1.41	1.73	1.41

Inter-class matrix

2.9	2.8	1.5	1.3	1.5
3.5	3.4	1.9	1.8	1.9
3.3	3.3	1.6	1.6	1.6
3.6	3.6	2.1	1.9	2.1
3.3	3.4	1.8	1.6	1.8

2.9	2.7	2.8	3.1	3.1
1.7	1.6	1.8	2.1	2.2
2.4	2.3	2.6	2.8	3
1.8	1.8	2	2.2	2.4
3	2.9	2.9	3.2	3.2

Cumulative Frequency Table (INTRA-CLASS)

Range	Frequency	CF	Probability
-0.3<x<=0	3	3	0.06
0<x<=0.3	8	11	0.16
0.3<x<=0.6	7	18	0.14
0.6<x<=0.9	6	24	0.12
0.9<x<=1.2	10	34	0.2
1.2<x<=1.5	8	42	0.16
1.5<x<=1.8	4	46	0.08
1.8<x<=2.1	2	48	0.04
2.1<x<=2.4	1	49	0.02
2.4<x<=2.7	1	50	0.02

Cumulative Frequency Table (INTER-CLASS)

Range	Frequency	CF	Probability
1<x<=1.4	1	1	0.02
1.4<x<=1.8	14	15	0.28
1.8<x<=2.2	9	24	0.18
2.2<x<=2.6	4	28	0.08
2.6<x<=3	10	38	0.2
3<x<=3.4	9	47	0.18
3.4<x<=3.8	3	50	0.06

2.4 Part 2 (Scatter matrices, Cumulative frequency table)

Intra-class matrix

1.5	1.6	1.1	1.3	1.4
1.2	1.4	0.7	0.9	1.1
1	1.2	0.6	0.9	1.1
1	1.2	0.7	0.7	0.9
0.7	0.8	0.8	0.8	1

2	2	2.2	2.5	2.2
2.2	2.2	1.4	1.7	2
2	1.4	1.7	2	1.7
2.2	1.7	1.4	1.7	1.4
1.4	1.4	1.7	2.5	2.2

Inter-class matrix

3.2	3	2.6	2.1	2.1
3.8	3.6	3.1	2.5	2.3
3.5	3.6	2.8	2.3	2.2
4	3.9	3.3	2.6	2.6
3.7	3.7	3.1	2.3	2.5

3.9	3.9	3.5	3.8	4
2.8	2.9	2.5	2.8	3
3.2	3.2	3	3.2	3.5
2.7	2.8	2.4	2.7	2.9
4	4	3.6	3.9	4.1

Cumulative Frequency Table (INTRA-CLASS)

Range	Frequency	CF	Probability
0.3<x<=0.6	1	1	0.02
0.6<x<=0.9	10	11	0.2
0.9<x<=1.2	9	20	0.18
1.2<x<=1.5	10	30	0.2
1.5<x<=1.8	7	37	0.14
1.8<x<=2.1	5	42	0.1
2.1<x<=2.4	6	48	0.12
2.4<x<=2.7	2	50	0.04

Cumulative Frequency Table (INTER-CLASS)

Range	Frequency	CF	Probability
2.0<x<=2.4	7	7	0.14
2.4<x<=2.8	12	19	0.24
2.8<x<=3.2	11	30	0.22
3.2<x<=3.6	7	37	0.14
3.6<x<=4.0	12	49	0.24
4.0<x<=4.4	1	50	0.02